



# High-Resolution Finger MRI: What Should You Look for in Trauma of the Fingers?

손가락의 고해상도 자기공명영상: 외상성 병변에서  
무엇을 봐야하는가?

Kyoung Yeon Lee, MD , Jiwon Rim, MD ,  
Jung-Ah Choi, MD\* , Eun Kyung Khil, MD

Department of Radiology, Hallym University Dongtan Sacred Heart Hospital, Hwaseong, Korea

## ORCID iDs

Kyoung Yeon Lee <https://orcid.org/0000-0003-2059-155X>

Jiwon Rim <https://orcid.org/0000-0001-5278-6496>

Jung-Ah Choi <https://orcid.org/0000-0002-0896-4766>

Eun Kyung Khil <https://orcid.org/0000-0002-7764-4344>

Received August 26, 2022  
Revised December 15, 2022  
Accepted May 6, 2023

## \*Corresponding author

Jung-Ah Choi, MD  
Department of Radiology,  
Hallym University Dongtan  
Sacred Heart Hospital,  
7 Keunjaebong-gil,  
Hwaseong 18450, Korea.

Tel 82-31-8086-2588

Fax 82-31-8086-2584

E-mail [jachoi88@gmail.com](mailto:jachoi88@gmail.com)

This is an Open Access article distributed under the terms of the Creative Commons Attribution Non-Commercial License (<https://creativecommons.org/licenses/by-nc/4.0>) which permits unrestricted non-commercial use, distribution, and reproduction in any medium, provided the original work is properly cited.

The fingers are among the most commonly injured structures in traumatic injuries resulting from sports and work. Finger injuries encompass a broad spectrum of injuries to bone and soft tissues, including tendons, ligaments, and cartilage. The high resolution of 3T MRI with dedicated surface coils allows for optimal assessment of the intricate soft tissue structures of the fingers. There have been several reports on detailed MRI features of the basic anatomy and common pathological findings of the finger and hand. Understanding the normal anatomy and familiarization with common traumatic lesions of the ligaments, tendons, and pulleys of the fingers on high-resolution MRI will allow radiologists to perform accurate preoperative evaluations of traumatic hand lesions. The purpose of this study is to review the normal hand anatomy and common traumatic lesions of the finger on high-resolution MRI and correlate them with surgical findings.

**Index terms** Fingers; Anatomy; Finger Injuries; Diagnostic Imaging; Magnetic Resonance Imaging

## INTRODUCTION

CT, MRI, and US can be used for preoperative evaluation of finger injuries. CT allows good assessment of bony structures and injuries; however, it is limited by its relatively low soft tissue resolution and possible radiation hazards. US is a safe and cost-effective tool for evaluating the superficial structures of the fingers, such as tendons, ligaments, nerves, and vessels (1). With the advancement of US technology, high-resolution probes with capacity for dy-

dynamic and Doppler imaging are additional benefits of this modality (2). However, the diagnostic performance of US depends on the operator's skills and the availability of high-resolution probes. 3T MRI with dedicated surface coils allows optimal depiction with spatial resolution of the soft tissue structures of the hand and fingers (3). Accurate preoperative assessment of traumatic finger lesions is needed, thereby allowing exact preoperative planning and effective treatment (4).

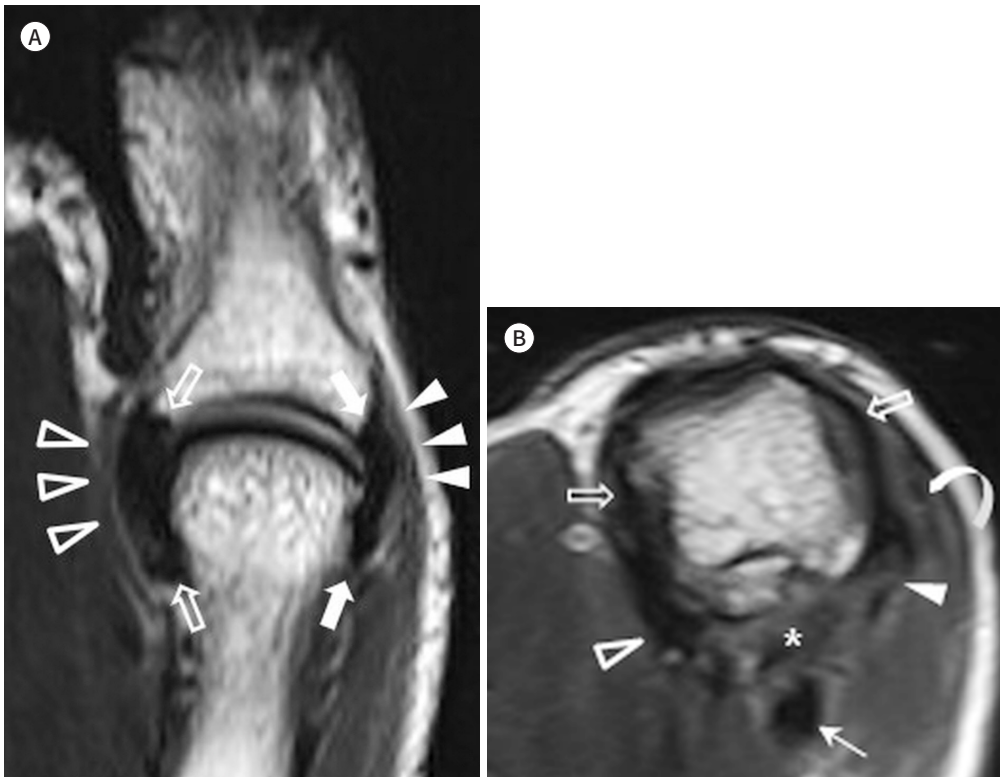
We used 3T MR scanners (Magnetom Verio and Skyra, Siemens Healthineers, Berlin and Munich, Germany) with 16-channel coils for hand and finger imaging. The MRI sequences included T1- and T2-weighted images in three planes with and without fat suppression.

In this pictorial review, we attempted to depict the normal anatomy and traumatic lesions of the ligaments, tendons, pulleys, extensor hood, and volar plate on high-resolution MRI using dedicated surface coils.

**Fig. 1.** Anatomy of the metacarpophalangeal joint of the thumb.

**A.** The T2-weighted coronal image shows the ulnar collateral ligaments (empty arrows) and the closely apposed, superficial aponeurosis of the adductor pollicis longus (empty arrowheads). A similar spatial relationship exists with the radial collateral ligament (arrows) and the superficial tendon of the abductor pollicis brevis (arrowheads).

**B.** The T2-weighted axial image depicts the main collateral ligaments (empty arrows), accessory collateral ligament (arrowhead), aponeurosis of the adductor pollicis longus (empty arrowhead), tendon of the abductor pollicis brevis (curved arrow), intersesamoid ligament (asterisk), and flexor pollicis longus tendon (thin arrow).



## ANATOMY OF THE THUMB

### LIGAMENTS

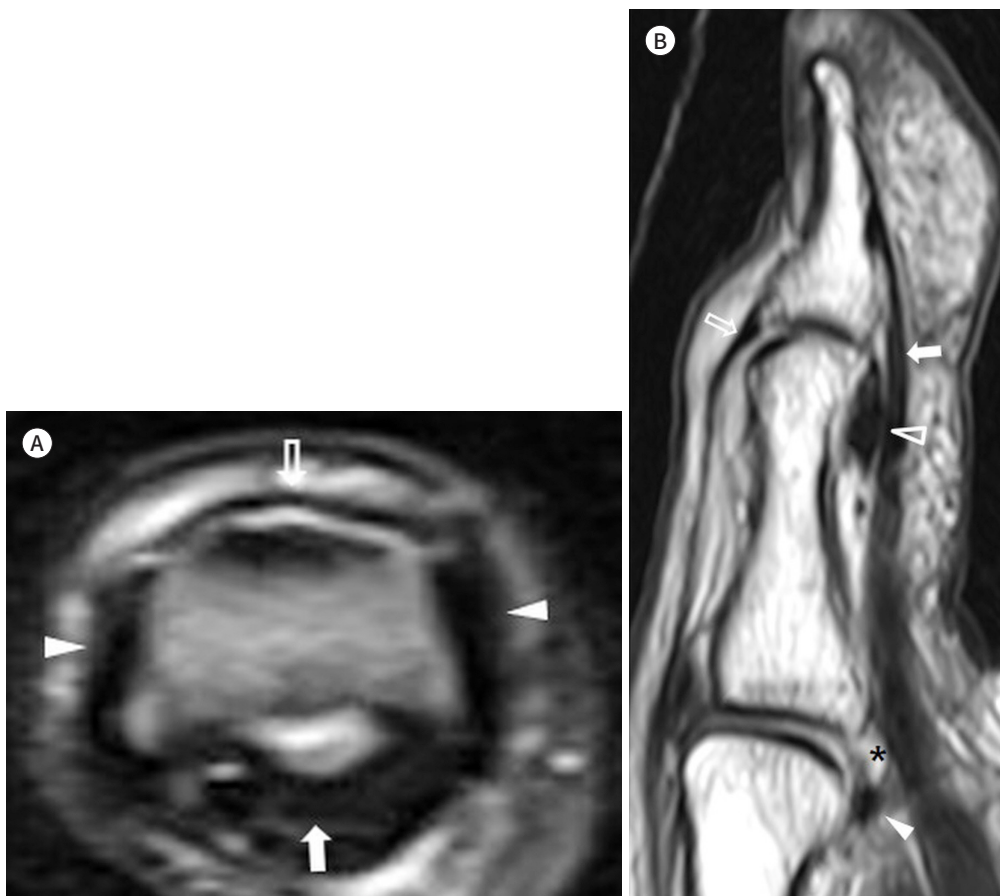
The radial collateral ligament (RCL) and ulnar collateral ligament (UCL) at the metacarpophalangeal (MCP) joint of the thumb are taut structures that stabilize the radial and ulnar aspects of the first MCP joint. The collateral ligaments attach to the distal margin of the first metacarpal bone and base of the proximal phalanx of the thumb. The UCL of the MCP joint of the thumb is covered by the superficial aponeurosis of the adductor pollicis longus (ADD) ventrally, and the RCL is covered by the superficial tendon of the abductor pollicis brevis dorsally (1, 4). On MRI, the collateral ligaments are located deep along the first MCP joint and appear as low signal intensity (SI) bands surrounded by vertically oriented aponeurosis of the ADD and abductor pollicis longus (ABD) tendons (Fig. 1).

The RCL and UCL at the interphalangeal (IP) joint of the thumb are similar to those at the MCP joint. These ligaments attach to the distal margin of the distal phalanx and head of the proximal phalanx, that stabilize the flexor pollicis longus (FPL) and extensor pollicis longus

**Fig. 2.** Anatomy of the interphalangeal joint of the thumb.

**A.** The T2-weighted axial image shows the collateral ligaments (arrowheads) as low signal intensity structures, flexor pollicis longus (arrow), and extensor pollicis longus tendons (empty arrow).

**B.** The T2-weighted sagittal image shows the insertion sites of the flexor pollicis longus (arrow) and the extensor pollicis longus (empty arrow) tendons, volar plate of the interphalangeal joint (empty arrowhead) and metacarpophalangeal joint (arrowhead), and adjacent sesamoid (asterisk).



(EPL) tendons (Fig. 2A).

### TENDONS AND THENAR MUSCULATURE

In the thumb, the FPL and EPL tendons attach to the tuft of the distal phalanx. On MRI, the insertion sites of the FPL and EPL are best visualized in the sagittal plane as low SI structures. In addition to the proximal and distal attachments, the volar plate of the thumb has

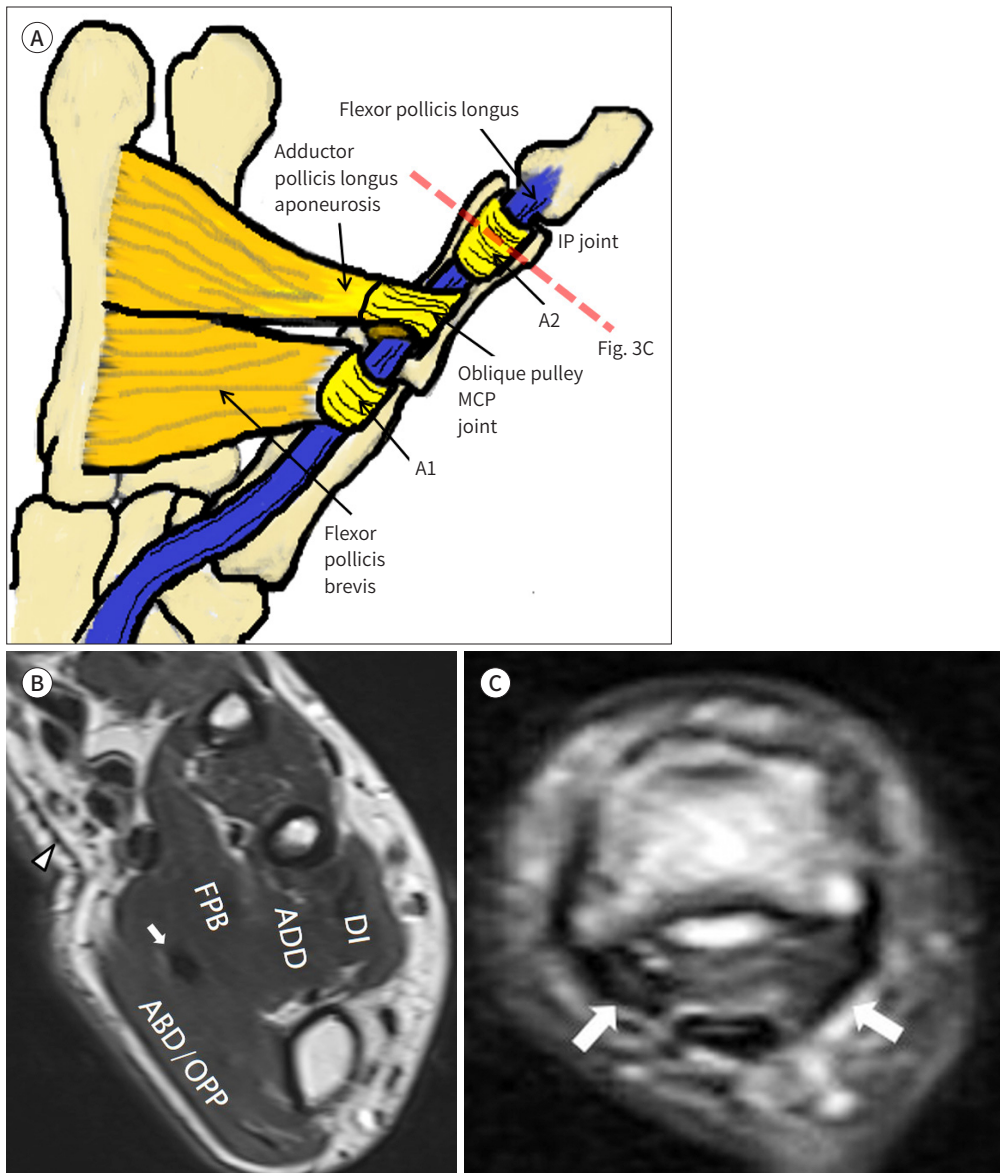
**Fig. 3.** Normal anatomy of the pulley system of the thumb.

**A.** The illustration of the thumb pulley anatomy shows two annular pulleys at the level of the metacarpophalangeal joint (A1) and interphalangeal joint (A2).

**B.** The DI, ADD, FPL and tendon (arrow), FBP, and ABD and OPP are shown well on the T2-weighted axial image. The OPP can be seen inserting into the central palmar fascia (arrowhead).

**C.** The A2 pulley (arrows) at the proximal phalanx level on the T2-weighted axial image.

ABD = abductor pollicis longus, ADD = adductor pollicis, DI = dorsal interosseous, FBP = flexor pollicis brevis, FPL = flexor pollicis longus, MCP = metacarpophalangeal, OPP = opponens pollicis



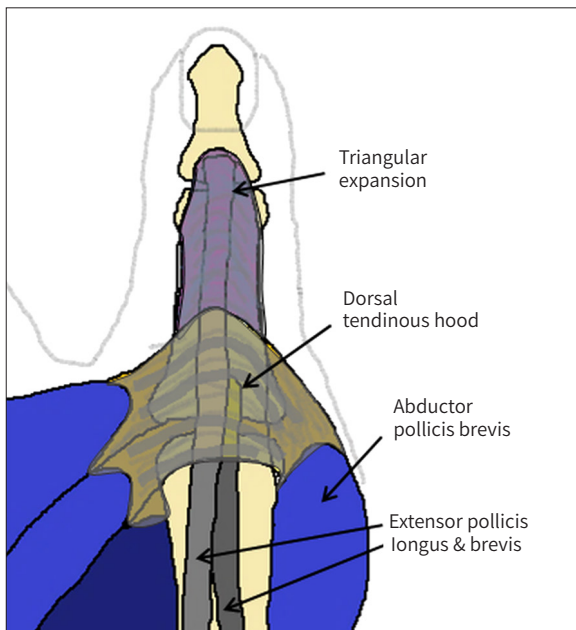


**Fig. 4.** Illustration of the thumb dorsal tendinous hood anatomy. The dorsal tendinous hood is located at the level of the first metacarpophalangeal joint and distally expanded as a triangular expansion for stabilizing the extensor pollicis longus/brevis tendons in the midline position.

two sesamoid bones embedded within (Fig. 2B) (1).

The thenar musculature consists of structures that mostly arise from the flexor retinaculum, such as the ABD, opponens pollicis (OPP), and flexor pollicis brevis (FPB). Although the ADD does not arise from the flexor retinaculum, it consists one of the thenar muscles (1). An interposed oblique pulley at the level of the proximal phalanx is closely associated with the attachment of the ADD aponeurosis (Fig. 3A). The ADD and dorsal interosseous (DI) are noted between the metacarpal bones. The FPL tendon is surrounded by smaller FPB bellies (Fig. 3B).

## PULLEYS

Two annular pulleys are located at the level of the MCP joint (A1) and first IP joint (A2). The oblique pulley is located between A1 and A2 at the distal aspect of the proximal phalanx. The variable annular pulley originates at the musculotendinous junction of the ADD and inserts at the radial side of the proximal phalanx (5). Axial MR sections at the proximal phalangeal base level reveal an A2 pulley (Fig. 3C).

## EXTENSOR HOOD

The extensor apparatus of the thumb consists of connective tissue for stabilizing the extensor pollicis brevis and EPL tendons in the midline position, and the dorsal tendinous hood is located at the level of the first MCP joint. The dorsal tendinous hood is distally expanded as a triangular expansion formed by oblique fibers (Fig. 4) (1).

## VOLAR PLATE

The volar plate surrounds the first MCP joint with intra-articular fibrous structures, reinforcing the volar plate and providing strength and stability to the joint capsule. The most common sesamoid bones in the hand are embedded in the volar plate of the first MCP joint.

They act as a pulley system by providing a smooth surface to the tendon to maximize mechanical force, promote dynamic directional movement, and reduce joint friction (1). The sagittal MR sections are the best for assessing the anatomy of the volar plates at the MCP and IP joints (Fig. 2B).

## ANATOMY OF THE LIGAMENTS AND FLEXOR AND EXTENSOR SYSTEMS OF THE FINGERS

Each collateral ligament complex consists of the main and accessory collateral ligaments. The main collateral ligament originates from the dorsolateral surface of the proximal bone, is oriented obliquely, and inserts into the ventrolateral surface of the base of the distal bone. The accessory collateral ligament is fan-shaped, originating ventral to the proper collateral ligament, and inserts into the lateral aspect of the base of the volar plate (6).

The collateral ligaments of the MCP joints attach proximally to the depressed portion of the lateral subcapital area of the metacarpal bone. There is a close spatial relationship between the superficial interosseous tendon and collateral ligaments. The continuous capsular structures include the sagittal bands, collateral ligaments, accessory collateral ligaments, and volar plates (Fig. 5).

The main collateral ligament, accessory collateral ligament, and volar plate stabilize the proximal interphalangeal (PIP) joint. The main collateral ligament inserts into the volar aspect of the middle phalangeal base and originates from the dorsal aspect of the proximal phalangeal head. The accessory collateral ligaments insert into the volar plate, which prevents hyperextension of the PIP joint due to the broad insertion of the middle phalanx (Fig. 6A) (7). The collateral ligaments at the PIP joint appear as linear low SI structures on MRI. The extrinsic tendons and the central and lateral slips contribute to the extensor mechanism (Fig. 6B).

The flexor tendons of the fingers consist of the flexor digitorum profundus (FDP) and flexor digitorum superficialis (FDS) (Fig. 7A). The FDP inserts into the distal phalangeal base and connects to the synovial sheath of the middle phalanx by the short and long vincula. The FDS tendon inserts into the middle phalangeal base and connects to the synovial sheath of the proximal phalanx by the short and long vincula. At the proximal phalangeal level, it splits into two, and the FDP passes through two separated portions of the FDS (8, 9). Axial MR images depict the tendons well from the proximal to the distal portions (Fig. 7B-D).

The extrinsic extensor tendon of the PIP joint consists of the central and lateral slips, which insert into the middle phalangeal base. The lateral slip merges with the intrinsic tendons, and the intrinsic tendons merge with the central slip. This crossing fiber pattern interconnects the central mechanism and intrinsic tendons (10). The middle phalangeal base, including the insertion site of the central and lateral slips, is best visualized on the median sagittal MR image (Fig. 8A). On the axial MR image, the extensor tendons show a low SI circumsccribing the dorsal aspect of the proximal phalanx (Fig. 8B).

The FDS and FDP tendons pass through the fibro-osseous canal, which consists of the palmar surface of the phalanges and the pulley system, to keep them closely approximated to the bone (8). The pulley system of the finger consists of a fibrous portion of the canal with five annular pulleys (A1–A5) and four cruciate pulleys (C0–C3) located from the distal phalangeal base to the metacarpal head of the finger (Fig. 9).

The extensor hood is a complex soft tissue network that stabilizes and limits proximal excursion at the level of the MCP joint, including the sagittal bands and transverse and oblique fibers of the interosseous hood. The main component of the extensor hood is a sagittal band,

**Fig. 5.** Normal anatomy of the collateral ligaments of the metacarpophalangeal joint of the second finger. **A.** The T2-weighted coronal image shows the collateral ligaments (arrows) attaching proximally in a depression of the lateral subcapital area of the metacarpal (arrowheads) with a close spatial relationship of the superficial interosseous tendon (empty arrows). **B.** The T2-weighted axial image shows the continuous nature of the capsular structures, including the sagittal bands (arrowheads), collateral ligaments (arrows), accessory collateral ligaments (empty arrows), and volar plate (asterisk).



**Fig. 6.** Normal anatomy of the collateral ligaments of the proximal interphalangeal joint of the third finger. **A.** The illustration shows the proximal interphalangeal collateral ligament anatomy of the third finger. **B.** The T2-weighted fat-suppressed coronal axial image shows the linear, low signal intensity appearance of the collateral ligaments (arrowheads), accessory collateral ligaments (arrows), volar plate (asterisk), central slip (empty arrow), and lateral slips (empty arrowheads) of the extensor mechanism.

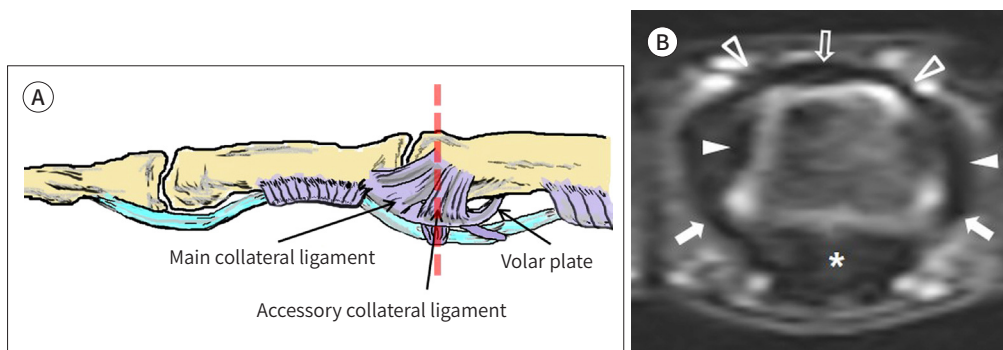


**Fig. 7.** Normal anatomy of the flexor tendon of the finger.

**A.** The illustration shows the flexor tendon anatomy of the third and fourth fingers.

**B-D.** The flexor tendon anatomy on the T1-weighted fat-suppressed axial MR images through the finger from the proximal to distal levels. The FDP tendon (asterisks) in a position dorsal to the FDS tendon (arrows) at the level of the metacarpals (**B**). The FDP tendon (asterisk) passing through a split in the FDS tendon (arrows) at the level of the proximal aspect of the middle phalanx (**C**). The FDP tendon (asterisk) palmar to the two separated portions of the FDS tendon (arrows) before insertion at the middle phalanx (**D**).

FDP = flexor digitorum profundus, FDS = flexor digitorum superficialis

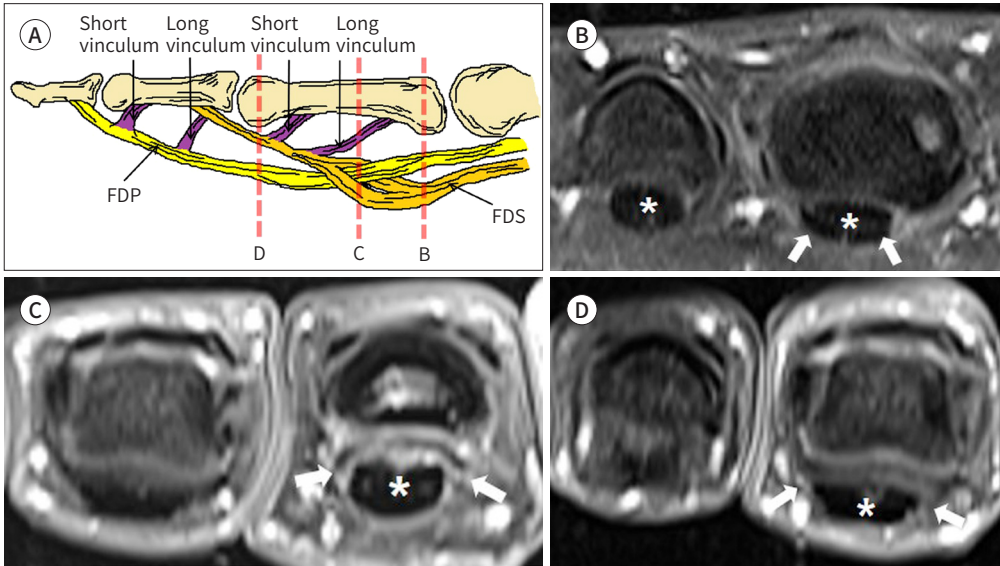


**Fig. 8.** Extensor tendon anatomy at the proximal interphalangeal joint.

**A.** The T2-weighted sagittal image delineates the extensor tendon anatomy with relation to the joint capsule. The central slip attachment to the base of the middle phalanx (arrow) and terminal tendon attachment to the base of the distal phalanx (arrowhead) are noted. The dorsal capsular recesses of both the proximal and distal interphalangeal joints are shown (empty arrows).

**B.** The T1-weighted axial image demonstrates the central slip attachment to the middle phalanx as well as the lateral slips (arrowheads) of the extensor tendon (arrow).

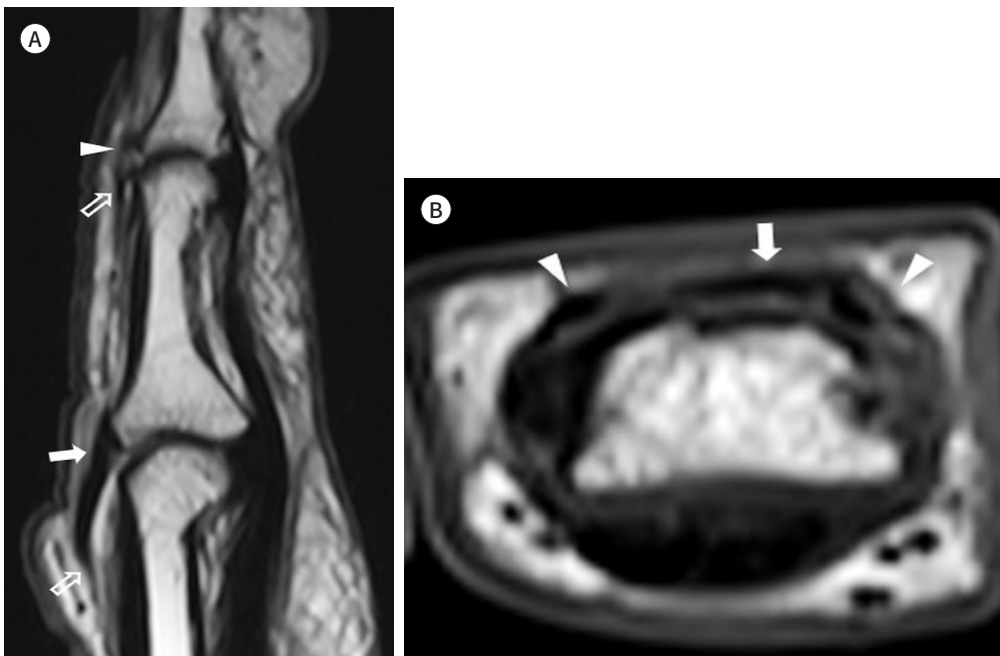


**Fig. 9.** Normal anatomy of the pulley system.

**A.** The illustration of the pulley system shows the annular pulleys (A1–A5) and cruciate pulleys (C0–C3).  
**B.** The T2-weighted axial image shows the A2 pulleys (arrowheads) of the second and third fourth fingers.  
 DIP = distal interphalangeal, FDP = flexor digitorum profundus, FDS = flexor digitorum superficialis, MCP = metacarpophalangeal, PIP = proximal interphalangeal

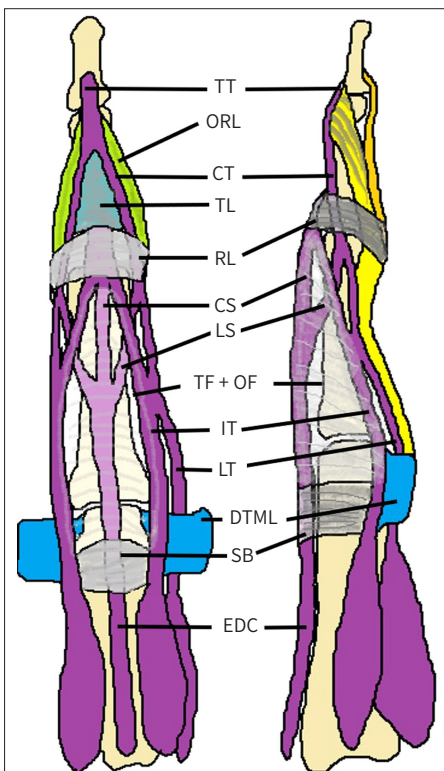
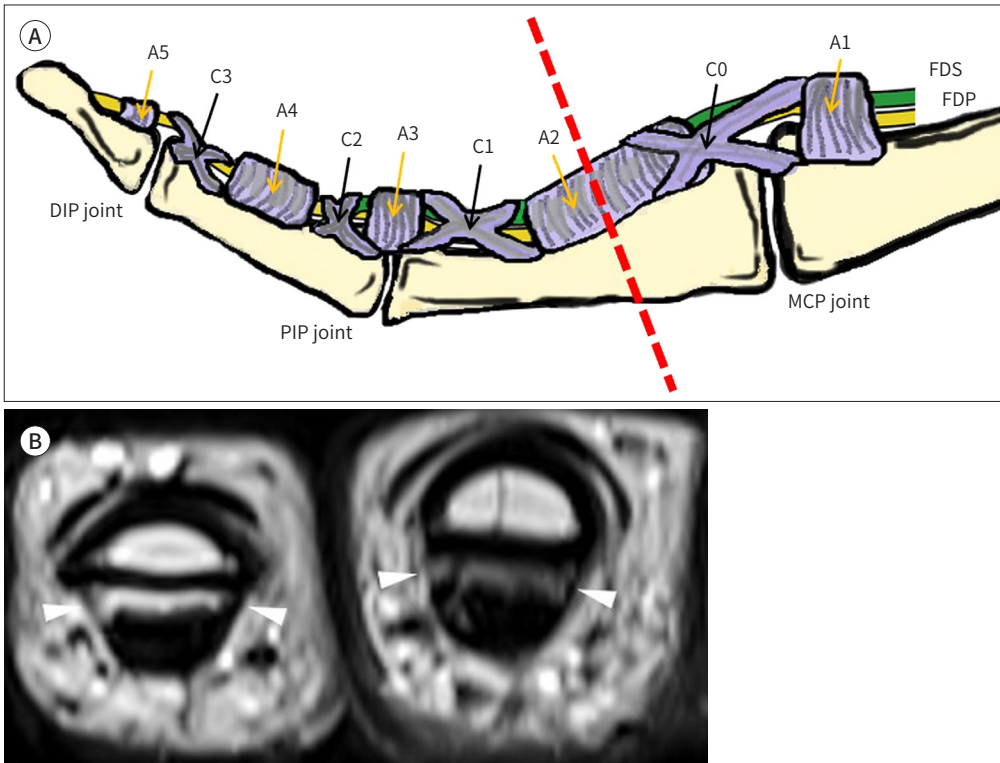


**Fig. 10.** The illustration of multiple soft tissue components that contribute to the extensor hood includes the EDC, SB, DTML, TF + OF, RL, TL, ORL, TT, CT, CS, LS, IT, and LT. CS = central slip, CT = central tendon, DTML = deep transverse metacarpal ligament, EDC = extensor digitorum communis, IT = interosseous tendon, LS = lateral slip, LT = lumbrical tendon, ORL = oblique retinacular ligament, RL = retinacular ligament, SB = sagittal band, TF + OF = transverse and oblique fibers of the interosseous hood, TL = triangular ligament, TT = terminal tendon

a capsular fibrous sheet that surrounds the MCP joint axially with a volar side attachment adjacent to the volar plate and a dorsal point of attachment to the extensor tendon (Fig. 10) (8).

The volar plate of the MCP joint is interconnected with the deep transverse MCP ligament and stabilizes the MCP head (7, 9). The normal bare area of the metacarpal bone is located between the articular surface and proximal capsular attachment. The volar plate of the IP joint consists of thick fibrocartilage tissue located at the palmar aspect of the joint capsules. The volar plate prevents hyperextension of the IP joint by attaching two lateral bands and stabilizing the central and lateral slips (Fig. 11) (9).

## INJURIES OF THE COLLATERAL LIGAMENTS, TENDONS, AND PULLEY SYSTEM

### COLLATERAL LIGAMENT INJURIES

Lesions of the UCL of the thumb usually occur at the distal insertion into the proximal phalanx and may be accompanied by bone avulsion. MRI findings include surrounding effusion, discontinuity of the distal portion of the UCL, and its rounded stump end (Fig. 12). In the case of Stener lesions, the torn UCL is retracted and lies superficial to the aponeurosis of



**Fig. 11.** Volar plate anatomy on the proximal and distal interphalangeal and metacarpophalangeal joints of the second finger. The T2-weighted fat-suppressed sagittal image shows the volar plate (arrowheads), distal recess of the volar plate (empty arrowheads), and distal extent of the dorsal recess (empty arrows). The normal bare area of the metacarpal (arrow) is noted between the articular surface and proximal capsular attachment.

the ADD (9).

Although injuries to the collateral ligaments of the other fingers are uncommon, they may occur on the radial side because of forceful ulnar deviation and may be associated with volar plate injury (11). MRI may show a discontinuity, detachment, or thickening of the injured ligament with edema or hemorrhage (Fig. 13) (9).

## TENDON INJURIES

The extensor tendon system consists of thin, superficially located structures that are prone to injury by laceration or avulsion (9). MRI of extensor tendon injuries may show adhesion or distortion of the injured tendons (Fig. 14).

Subluxation or dislocation of the extensor tendons may be accompanied by tears in the sagittal bands of the extensor hood (9). MRI may show an abnormal position of the extensor tendon and extensor hood injuries with findings of poor definition, focal discontinuity, and focal thickening of the injured tendons (Fig. 15).

Lesions of the flexor tendon system are less common than those of the extensor tendon system. It occurs more frequently in the midsubstance areas than at bony insertion sites (9). MRI may show tenosynovitis, disruption, and discontinuity of the injured tendon. As retraction of the injured tendon occurs, the gap between the tendon ends is well shown on MRI (Fig. 16).

**Fig. 12.** Complete tear of the UCL of the thumb.

**A, B.** The T2-weighted fat-suppressed coronal images in a 33-year-old female with right thumb injury show discontinuity of the proximal portion of the torn UCL of the thumb metacarpophalangeal joint (arrows). UCL = ulnar collateral ligament

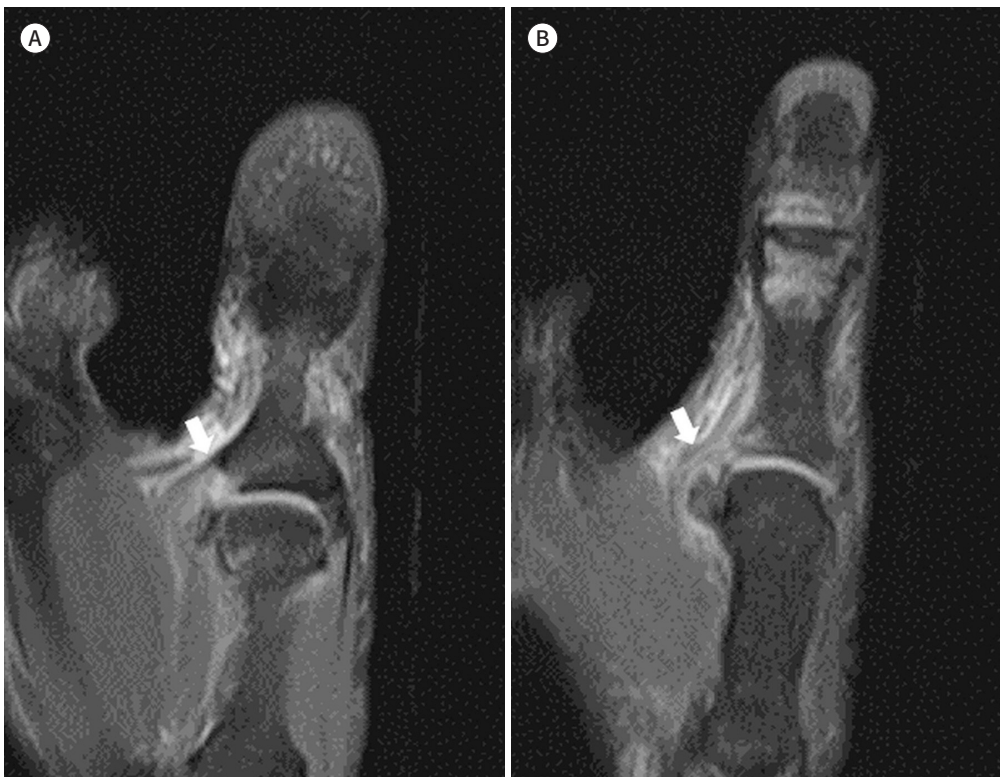
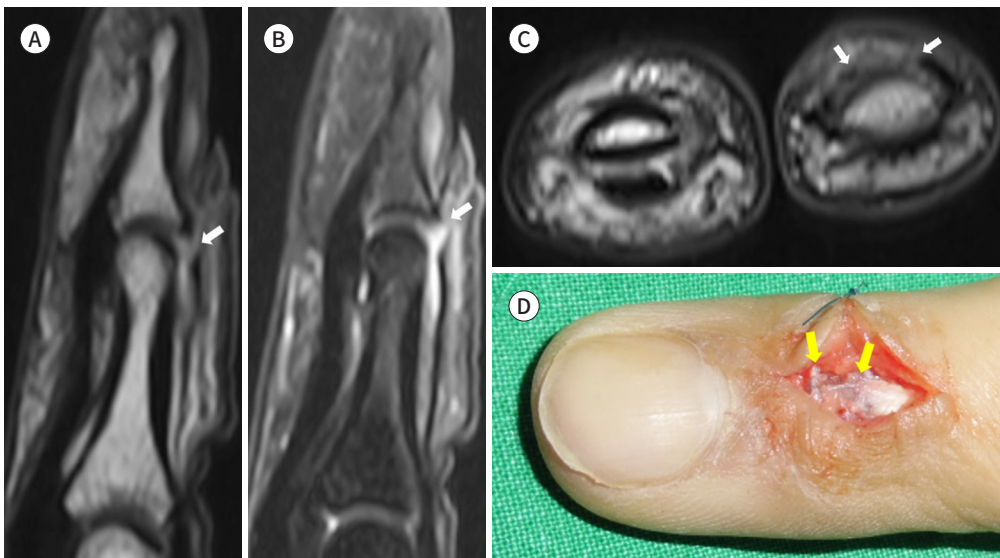




**Fig. 13.** Complete tear of the UCL of the third finger. **A, B.** The proton density-weighted fat-suppressed coronal (**A**) and axial (**B**) images in a 45-year-old female with right third finger injury by fall while riding a horse show discontinuity of the UCL of the right third finger proximal interphalangeal joint at the distal insertion and avulsion fracture at the right third distal phalangeal base (arrows). UCL = ulnar collateral ligament

**Fig. 14.** Complete tear of the extensor digitorum tendon of the second finger. **A-D.** The T2-weighted sagittal images without (**A**) and (**B**) with fat suppression and T2-weighted axial images (**C**) in a 20-year-old male with right second finger injury by a cutter knife show detachment of the right second finger extensor digitorum tendon at the distal insertion site (arrow in **A, B**, arrows in **C**); on surgery, the findings are correlated with a gross photograph (arrows in **D**).



### PULLEY SYSTEM INJURIES

Injuries to the pulley system result from extensive flexion of the fingers with extension of the MCP, flexion of the PIP, and extension of the distal interphalangeal joints, which may cause excessive stress on the A2 and A3 pulleys, leading to eventual rupture (8, 9). MRI may show discontinuity, detachment, retraction, and perilesional edema (Fig. 17). In addition, the lesions of the pulley system can be diagnosed indirectly through the “bowing sign,” which is a gap be-

**Fig. 15.** Subluxation of the extensor pollicis longus and brevis tendons of the thumb.  
A-C. The T2-weighted sagittal (A) and axial (B, C) images in a 62-year-old-female with right thumb injury by slip down show subluxation of the extensor pollicis longus and brevis to the ulnar side with thinning of both tendons (arrows).

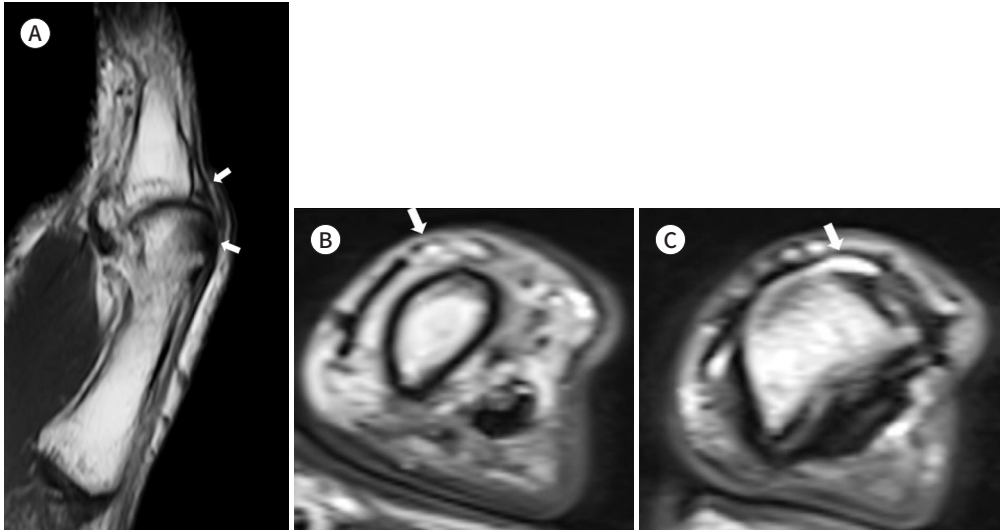
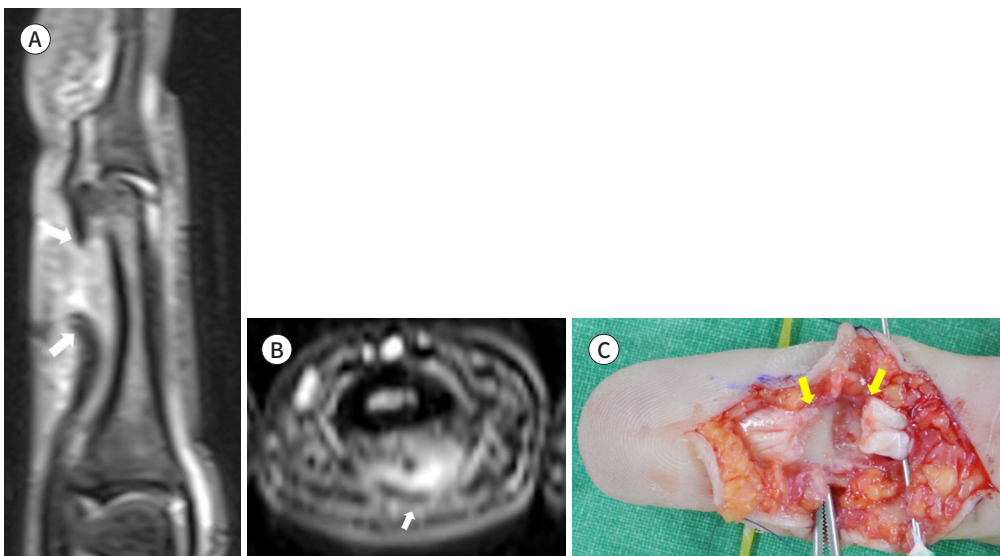


**Fig. 16.** Complete tear of the flexor digitorum profundus tendon of the third finger.  
A-C. The T2-weighted fat-suppressed sagittal (A) and axial (B) images in a 21-year-old-female with right third finger injury cut by a piece of glass show detachment and retraction of the third finger flexor digitorum profundus tendon at the middle phalanx distal portion with a gap between the tendon ends (arrows); on surgery, the findings are correlated with a gross photograph (C).



tween the bone and flexor tendon on sagittal images obtained during flexion (Fig. 18) (9).

## CONCLUSION

Knowledge of the normal anatomy and typical traumatic lesions of the fingers on high-res-

**Fig. 17.** Rupture of the C1 pulley of the second finger.

**A, B.** The T2-weighted fat-suppressed sagittal (**A**) and axial (**B**) images in a 35-year-old male with right second finger injury while playing soccer show detachment (arrow) and retraction (arrowhead) of the right second finger C1 pulley.

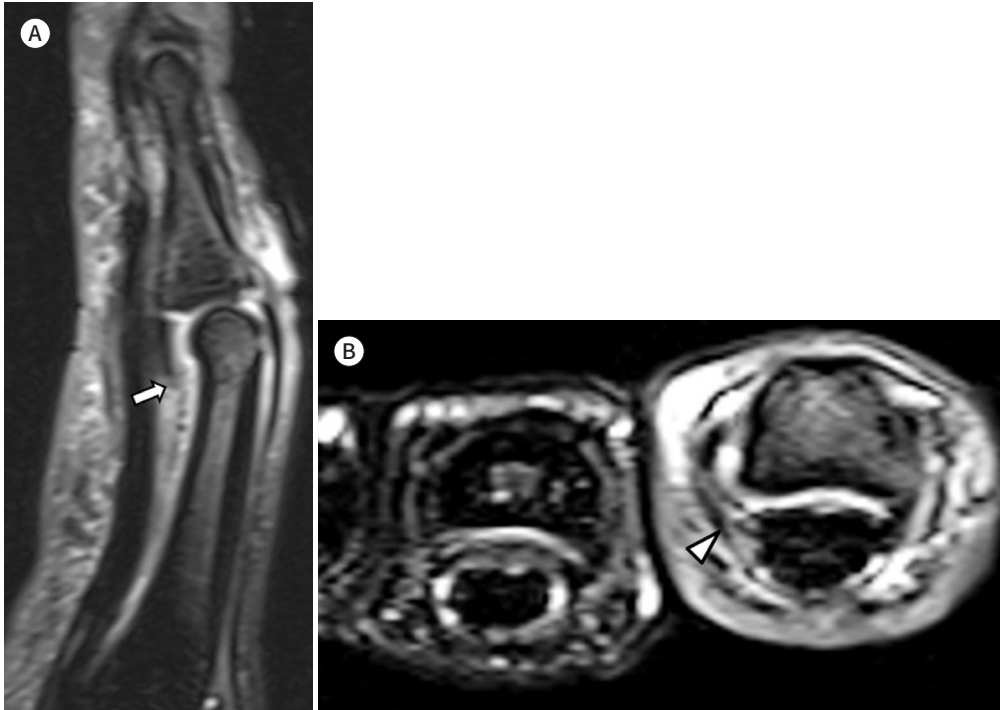
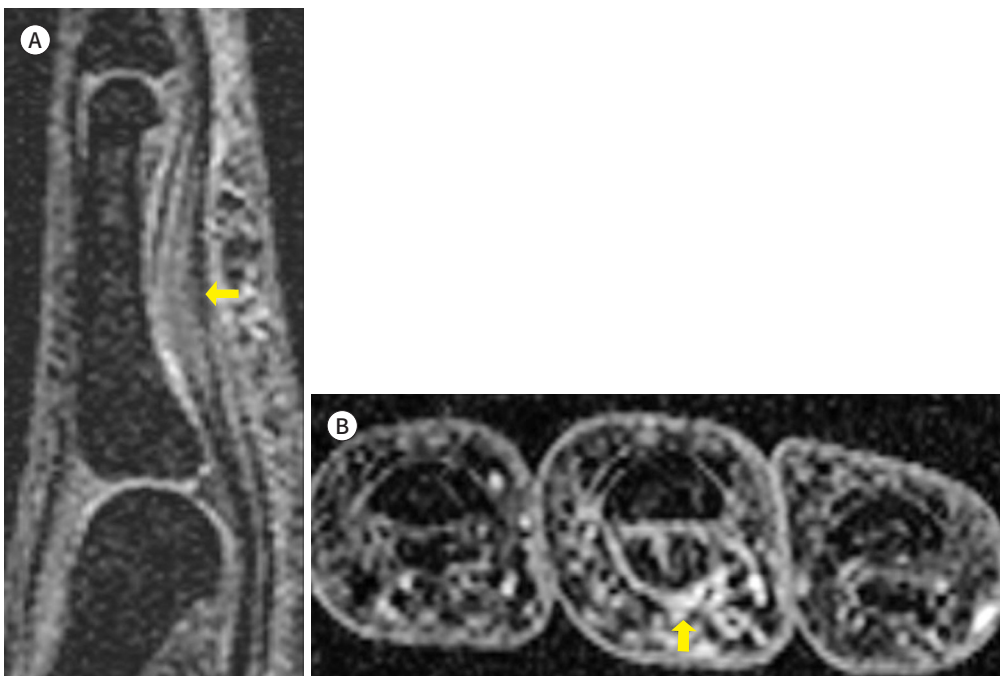


**Fig. 18.** Rupture of the A2 pulley of the third finger.

**A, B.** The proton density-weighted fat-suppressed sagittal (**A**) and axial (**B**) images in a 36-year-old male with spontaneous pain in the left third finger show increased signal intensity and discontinuity of the A2 pulley of the third finger at the proximal phalanx level (arrows) without a significant gap between the middle phalangeal bone and flexor tendon.



olution MRI allows radiologists to make accurate preoperative diagnoses for the precise preoperative planning and treatment of injuries.

### Author Contributions

Conceptualization, R.J., C.J.; data curation, R.J., C.J., K.E.K.; formal analysis, R.J., C.J.; investigation, L.K.Y., C.J.; methodology, L.K.Y., C.J.; supervision, C.J.; validation, L.K.Y., C.J.; visualization, C.J., K.E.K.; writing—original draft, all authors; and writing—review & editing, all authors.

### Conflicts of Interest

The authors have no potential conflicts of interest to disclose.

### Funding

None

### Acknowledgments

This study has been approved by the institutional review board.

## REFERENCES

1. Rawat U, Pierce JL, Evans S, Chhabra AB, Nacey NC. High-resolution MR imaging and US anatomy of the thumb. *Radiographics* 2016;36:1701-1716
2. Lee SA, Kim BH, Kim SJ, Kim JN, Park SY, Choi K. Current status of ultrasonography of the finger. *Ultrasonography* 2016;35:110-123
3. Major NM, Anderson MW, Helms CA, Kaplan PA, Dussault R. *Musculoskeletal MRI*. 3rd ed. Amsterdam: Elsevier 2020:263-294
4. Baz AAM, Hussien AB, Samad HMA, El-Azizi HMS. Diagnostic performance of high-resolution ultrasound in pre-and postoperative evaluation of the hand tendons injuries. *Egypt J Radiol Nucl Med* 2021;52:6
5. Hirschmann A, Sutter R, Schweizer A, Pfirrmann CW. MRI of the thumb: anatomy and spectrum of findings in asymptomatic volunteers. *AJR Am J Roentgenol* 2014;202:819-827
6. Craig SM. Anatomy of the joints of the fingers. *Hand Clin* 1992;8:693-700
7. Petchprapa CN, Vaswani D. MRI of the fingers: an update. *AJR Am J Roentgenol* 2019;213:534-548
8. Ragheb D, Stanley A, Gentili A, Hughes T, Chung CB. MR imaging of the finger tendons: normal anatomy and commonly encountered pathology. *Eur J Radiol* 2005;56:296-306
9. Clavero JA, Alomar X, Monill JM, Esplugas M, Golanó P, Mendoza M, et al. MR imaging of ligament and tendon injuries of the fingers. *Radiographics* 2002;22:237-256
10. Clavero JA, Golanó P, Fariñas O, Alomar X, Monill JM, Esplugas M. Extensor mechanism of the fingers: MR imaging-anatomic correlation. *Radiographics* 2003;23:593-611
11. Jarvik JG, Dalinka MK, Kneeland JB. Hand injuries in adults. *Semin Roentgenol* 1991;26:282-299

## 손가락의 고해상도 자기공명영상: 외상성 병변에서 무엇을 봐야하는가?

이경연 · 임지원 · 최정아\* · 길은경

손가락은 일상생활과 스포츠 활동 중에 가장 흔하게 손상될 수 있는 구조물이다. 손가락 손상은 손가락의 뼈와 인대, 연골을 포함한 연부조직까지 다양한 구조물의 손상을 포함한다. 특수 표면코일을 이용한 고해상도 3 테슬라 자기공명영상을 이용하여 복잡한 연부조직 구조물들을 평가할 수 있다. 손가락과 손의 기본 해부학과 흔한 병변의 자기공명영상 소견들에 대한 기존의 보고들이 있다. 손가락의 인대, 건, 도르래 등 여러 구조물의 기본 해부학과 흔한 외상성 병변의 영상학적 소견의 이해는 다양한 손의 외상성 병변에 대한 정확한 평가를 가능하게 한다. 본 논문에서는 손가락의 기본 해부학적 구조 및 흔한 외상의 자기공명영상 소견을 복습하고, 실제 수술장 소견과 연관 지어 이해를 돕고자 한다.

한림대학교 동탄성심병원 영상의학과